Cold Flow Simulations for a Pulse Detonation Rocket Ejector

J. Tyler Nichols, Donald R. Wilson, Frank K. Lu
Aerodynamics Research Center, Mechanical and Aerospace Engineering Department
University of Texas at Arlington, Arlington, TX 76019, USA

Abstract

This paper reports an exploratory experimental cold flow test of the first mode in a multi-mode propulsion concept. A small model of a wall-mounted pulse detonation rocket (PDR) ejecting into a duct was fabricated and integrated into the supersonic wind tunnel at the University of Texas at Arlington (UTA). Although supersonic testing proved to be inconclusive, the static tests showed that pulsed flows entrain more mass than steady state flows. It also indicated that thrust augmentation is more favorable at low frequencies for this model.

Background

Pulse detonation engines (PDE) have been researched extensively as an alternate form for high-speed propulsion. A concept has been proposed for the adaptation of a PDE into a type of scramjet in which the PDE ejects into a subsonic or supersonic secondary flow to provide thrust. A model of such a configuration was developed and tested in the supersonic blow-down tunnel at the Aerodynamics Research Center (ARC) at the University of Texas at Arlington (UTA). This was done as a means of determining if this is a viable option for future propulsion.

The first step is to conduct "cold-flow" simulations in which the gas cycles in the PDE chamber are left undetonated to provide a baseline for future experiments. As a means of safety, atmospheric air is used to replace the fuel and the oxidizer since there is no combustion. That is the basis for this research and thesis.

Multi-mode Propulsion Concept

In the National Aerospace Plane program, as well as other hypersonic vehicle proposals, one of the major obstacles that must be overcome is the development of a propulsion system that can transition between all flight regimes. A propulsion system for this type of application is needed to start at rest, accelerate through the transonic region, and continue to accelerate to a hypersonic cruise or even escape the sensible atmosphere.

One novel approach to solving this problem is a multi-mode propulsion concept proposed in Munipalli et al. [1]. This system proposed takes advantage of ejectors and detonation physics as a means of providing thrust. This system operates with four distinct modes (Fig 1) as shown below.

(1) An ejector augmented pulsed detonation rocket for take off to moderate supersonic Mach numbers

(2) A pulsed normal detonation wave mode at combustion chamber Mach numbers less than the Chapman-Jouguet Mach number,

(3) An oblique detonation wave mode for Mach numbers in the air-breathing regime that are higher than the Chapman-Jouguet Mach number, and

(4) A pure pulsed detonation rocket (PDE) mode of operation at high altitude.

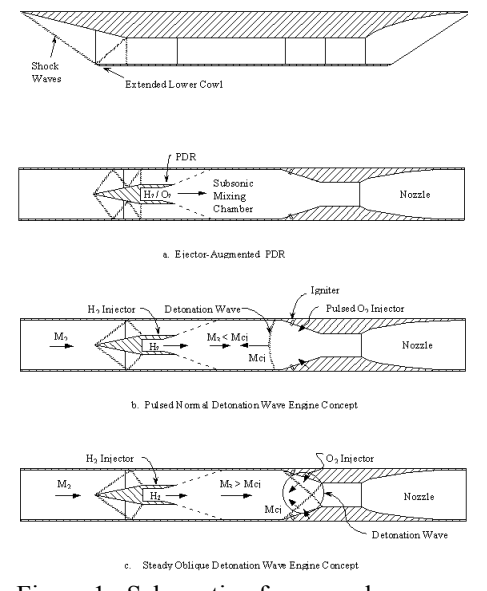

Figure 1: Schematic of proposed multimode engine

The obvious advantage to this is all modes can make use of the same internal geometry, eliminating the need for additional flow paths. Another benefit is the atmospheric air entering the duct does not have to be slowed to subsonic speeds at higher Mach numbers. This greatly reduces the losses in total pressure associated with shock waves and, in turn, increases efficiency. Shock waves also increase the static temperature, and without them, the gas

temperature can be maintained below the fuel auto-ignition temperature.

A great number of these concepts have not been explored, but the first mode will be the main focus of the experiments represented here.

Thrust Augmentation with Unsteady Flow

One of the primary measures of performance for an ejector is the thrust augmentation associated with it. Thrust augmentation is defined as the ratio of thrust from the mixed flow of an ejector and a ducted inlet flow to the thrust of the ejector alone. Mathematically, thrust augmentation is expressed by the following equation.

$$\Phi \equiv \frac{F_{Total}}{F_{Ejector}} \qquad (1)$$

An alternate means of determining thrust augmentation for steady-state ejectors arises in Porter and Squyers [3] in which it is posed in terms of the ratio of specific heats (γ), and the ratio of entrainment mass flow to jet mass flow (β).

$$\Phi = \left[1+\beta\right]^{(\gamma-1)/\gamma} \qquad (2)$$

The jet mass flow referred to in β is the same as the primary mass flow, and at rest, the entrainment mass flow can be taken to be the secondary mass flow. If this equation is applied to unsteady devices, it would be a function of values that fluctuate according to the unsteady nature of the device, but the complexity of the problem is greatly reduced as there are only two parameters that need to be determined: the primary mass flow and the secondary mass flow. In the experiments explored by Paxson and Wilson [4], it is found that this equation is fairly optimistic when compared to unsteady experimental data, yielding larger values than are actually seen. The disparity between actual and predicted values grows as β is increased. It does, however, provide a rough approximation for thrust augmentation when much of the flow information is not known.

Studies have found that unsteady ejectors have more favorable thrust augmentations than steady-state devices. In fact, thrust augmentation ratios as high as 1.8 have been seen in unsteady ejectors according to Paxson and Wilson [4]. It is the hope of this research to find this same trend in performance for unsteady-state ejectors that have a supersonic secondary flow.

Ejector Model

The model for this experiment consists of a single wall-mounted pulse detonation chamber that ejects into a supersonic inlet. Aft of that is a long duct where these flows can mix. Static pressure taps have been added as a means of sampling the conditions the model is experiencing at crucial locations.

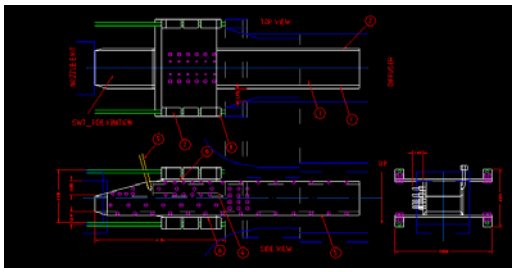

Figure 2: Three-view sketch of ejector model

Overall, the ejector is 30.0 inches long, 4.0 inches wide, and 3.125 inches tall.

The PDE chamber itself has a 1-inch by 4-inch cross-section, and is 8.0 inches long. Four static pressure taps are positioned directly along the centerline of the chamber and are spaced evenly, 2.0 inches apart from one another. The splitter plate that separates the PDE chamber from the secondary flow is tapered to a sharp point at the interface.

This chamber implements a front-wall injection of fuel and oxidizer from an array of cross-flow ejector ports. Fuel enters from one side, the oxidizer enters from the other, and both gases fan out into the chamber in opposite directions as a means of enhancing the mixing characteristics. There are a total of five injectors on each side that fan in 15-degree increments from the axial direction at the edges to 60.0 degrees off-axial in the center. Both the fuel and oxidizer are fed to the system via two 3/8-inch stainless steel lines. Purge air comes in the remaining ¼-inch stainless steel line in the center, and has two injectors independent of the fuel and oxidizer for it as well.

The two remaining holes on the front wall of the chamber are to accommodate the ignition system. These holes go through the base wedge to a small trough on the outside of the engine that can be easily accessed.

The model inlet is straight with constant area. This was done to insure that the secondary flow for high-speed testing is supersonic.

The duct is 14.75 inches from the front to the mixing interface. It is 4.0 inches wide and 1.75 inches tall. Seven pressure taps were installed every 2.0 inches down the system starting 1.75 inches aft of the front of the model.

The mixing interface is a simple, constant area duct. It makes up the last 16.0 inches of the model and is 4.0 inches in width and 3.125 inches in height. The most significant feature of

the mixing interface is the matrix of pressure taps that sit just aft of the splitter plate where the primary and secondary flow merge. This matrix was added to examine the interaction of the two flows. The matrix consists of twelve taps arranged in four rows of three and starts 1.25 inches beyond the splitter plate. The taps are spaced on 1-inch centers front to back and 0.75-inch centers top to bottom. This leaves the top and bottom taps 0.375 inches from the inner top and bottom walls of the model.

Control System

The main components of the control system consist of a remote control box in the control room, a control cart, a rotary valve system, and an umbilical electrical cable for communication between all components and the control room.

Pulsating the flow for this experiment was done with a rotary valve driven by an electric motor. This entire assembly was fixed to the bottom of the supersonic wind tunnel keeping the cyclical flow lines downstream of the valve as short as possible so the time delays of the pulsing air would be kept to a minimum.

The rotary valve itself is a 1.5-inch shaft with 19/64-inch holes drilled through the axis. Due to symmetry, the valve opens and closes twice per revolution of the shaft making the pulsating gas frequency exactly twice that of the rotary valve. The rotary valve was originally designed with accommodations for six supply lines. For this experiment, the valve was adapted to only use three of these lines, one for fuel, oxidizer, and purge air. Since purge air is needed to provide a buffer between detonations, the holes on the rotary valve are drilled 90 degrees out of phase, equating to a purge air pulse that is 180 degrees out of phase with the primary fuel and oxidizer pulse.

The rotary valve is driven by a 1/2 hp electric motor via a timing belt. Both the rotary valve and the motor have teeth to prevent slipping. The motor has also been retrofitted with a variable resistor controller that allows the motor to be set at different speeds. This was the way pulse frequency was varied in the experiments. Because this resistor was mounted directly to the motor, motor frequency, and, ultimately PDE frequency, could not be adjusted remotely. These presets all had to be set prior to the experiments. Due to the fact that this was simply an analog dial control, pulse frequency could not be set to an exact, reproducible value each time. Fortunately, the frequency of the system can be retrieved from the data being collected to an accuracy on the order of the sampling rate.

As stated earlier, most of the PDE controlling devices were mounted on a portable cart. This allows future experiments to use this same control system. The primary functions of the control cart are to open and close valves for the fuel, oxygen, and purge air.

Due to the fact that highly combustible gases were regulated with the control cart, pneumatic valves that were driven with shop air were used in the main supply path. The pneumatic valves used were designed to service a ½ inch supply line. Three of these valves were needed for the fuel, oxidizer, and purge air. Flow meters were also installed on the fuel and oxidizer lines for later research. Four feet of flexible ½ inch supply hose was used to connect the cart to the supply sources and the rotary valve assembly under the wind tunnel.

For the shop air that drives the pneumatics, a ¼ inch copper supply line ties the pneumatic valves to the solenoid valves on the opposite side of the cart. This allows all of the electrical systems to be as isolated from the flammable gases as possible.

Also on the opposite side of the cart is the power supply for the solenoid valves. It has a few manual controls for operating the valves at the top and fuses for each of the individual solenoid circuits.

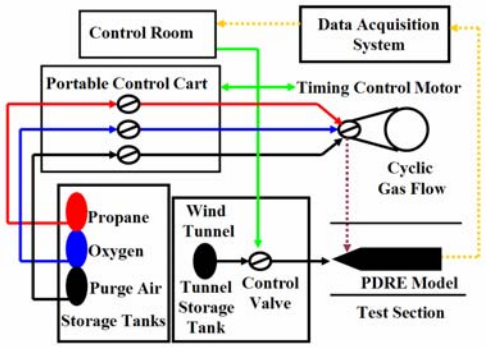

Figure 3: Illustration of experimental setup

Wind Tunnel

The wind tunnel used is a sub-scale supersonic blowdown tunnel that has been integrated into the ARC at UTA. This tunnel has a range of Mach 1.5 to 4 and a run time of at least 2 seconds according to Matsumoto [6].

The tunnel itself is fairly straightforward. There is a storage tube that extends out the front, followed by both a manual safety valve and a computer controlled pneumatic driver valve. Beyond the valves is a plenum chamber that is

meant to condition the flow and eliminate any minor fluctuations that may be experienced. After that, the flow enters an adjustable converging-diverging (CD) nozzle that can accelerate the flow through the sonic point to the desired test section Mach number. The test section sits just aft of this, followed by a long diffuser. The test section is 0.15 meters by 0.15 meters, and the model, as mentioned, was designed around this constraint. The test section can also be unbolted from the nozzle and slid back for access to models and test equipment.

The wind-tunnel has a separate, lower-frequency data acquisition system to monitor pressure in the storage tube, plenum chamber, and test chamber as well as temperature in the plenum chamber. The only control mechanism on the wind tunnel is the automatic valve. Both the valve control and data acquisition were done from a single computer in the control room. Matsumoto [6] details the computer code that is used to drive the valve for uniform flow during tests.

Modifications for Cold Flow

Due to the fact that this set of experiments are all cold flow simulations in which the gas is not to be detonated, a few modifications needed to be made to the experiment.

As stated earlier, the fuel and oxidizer supplies were replaced with atmospheric air for safety. The PDE chamber will not have any detonation to drive the flow supersonic in a cyclical manner. A wedge was made to fit at the opening of the PDE chamber to do this. To ensure that there is sonic choked flow at the throat, the cross-sectional area at the throat must be smaller than the entire flow path upstream. Because the model has is a fixed width of 4.0 inches, the height of the throat must be 0.025 inches to meet this criteria.

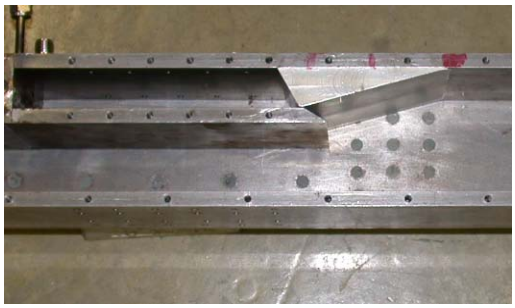

Figure 4: Model retrofitted with a CD nozzle

The slope on the diverging part of the wedge was maintained at 15.0 degrees. In addition to this, the ports for the ignition system on the model had to be plugged as well in order to ensure that the entire flow in the PDE chamber exited through the nozzle into the mixing interface.

The rotary valve was also modified to allow the purge air line to open in phase with the fuel and oxidizer lines instead of 90 degrees out of phase. This was done as a means of increasing the mass flow per cycle and to eliminate any minor secondary pulses that might complicate the flow interpretation.

Runs Conducted

Because the tests are interested in seeing if this mode can accelerate from rest to supersonic conditions, it was important to perform a set of runs at each of these conditions. Also, it was important to see what effect varying the frequency of the PDE cycle would do to performance. With these conditions to explore, a system of five runs was conducted.

The first three runs were a steady-state, low frequency, and high frequency static test. In these tests, the test section was unbolted from the nozzle and detached to allow the engine to breathe properly while the wind tunnel was off.

The last two tests were low and high frequency tests of the model at supersonic conditions. The motor was varied in the same manner as before, but in these tests, the wind tunnel was used to simulate supersonic flight.

After the data was filtered and converted to "psig," it was converted to a pressure ratio using an ambient pressure reading from a barometer the day of the experiment. The convenience of manipulating the data in this fashion will be seen as the analysis is conducted. In the transducer data that is to follow, it is important to note that the lowest number represents the transducer that is the furthest upstream.

$$\frac{p_{static}}{p_{amb}} = \frac{p_{trans} + p_{amb}}{p_{amb}} \qquad (3)$$

Mach 0 Steady-state Run

For the steady-state run, the data acquisition system was also turned on prior to the activation of the control motor so as to capture the total response of the system to the step input from the ejector. A total of 5.12 seconds of run time was collected, but after filtering, only 4.32 seconds of run time was valid.

From the data gathered in the PDE, the transducers show that the system has a slightly under-damped second-order response to the motor activation. Once the transient response has decayed, the averaged pressure ratio from the

last three transducers of 2.18 remains. The first was not used because of the lack of correlation to the other three. Because the chamber to throat area ratio is 40.0, it can be assumed that the static pressure readings inside the chamber are close to stagnation values. This claim is validated by the fact that all transducers experience a pressure rise simultaneously when the flow is initiated. Even though the transducers do not agree on a final value, this uniform reaction suggests that the PDE chamber is acting more like a storage tank than an open-ended duct.

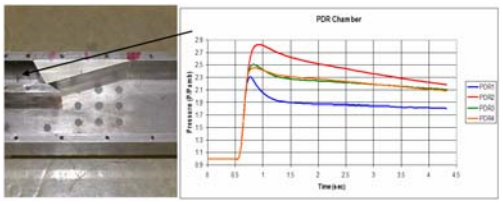

Figure 5: Static steady state PDE readings

On the diverging section of the nozzle, the final area ratio (A/A^*) at the perpendicular plane of the splitter plate is 22.96. Mattingly [8] shows that for expansion ratios on this order, there is a sonic condition at the throat for nozzle pressure ratios (NPR), $p_{chamber}/p_{ambient}$ only slightly greater than 1.0. Unfortunately, this text also indicates that there are shocks that form inside the nozzle slowing the flow to subsonic conditions for an NPR less than 14.0. This is a rather large expansion for such a low pressure ratio driving the flow, and it is anticipated that the flow is highly over-expanded. The flow experiences a shock somewhere in the nozzle to recompress it back to the exhaust pressure. Unfortunately, this indicates that the rest of the experiment aft of this location is subsonic as the cross-sectional area continues to grow.

To look at the primary mass flow, the mass flow equation must be applied to a point in the primary stream where the flow conditions are known. The obvious choice is the throat of the CD nozzle. Even though the flow conditions are not known at this point, it is assumed that the flow is choked at this location and flow properties can easily be determined from upstream flow properties. Recall the following equations for determining mass flow and speed.

$$\dot{m} = \rho V A \qquad (4)$$

$$V = M\sqrt{\gamma R T} \qquad (5)$$

Unfortunately, the flow properties at the throat are not known, so an alternate form of extracting this information is needed that relates the mass flow at this point to flow properties upstream. The mass flow parameter (MFP) as seen in Mattingly [8] does that by relating the mass flow at a given Mach number to total pressure and total temperature.

$$MFP(M) \equiv \frac{\dot{m}\sqrt{T_t}}{P_t A} = \frac{M\sqrt{\gamma/R}}{\left\{1+[(\gamma-1)/2]M^2\right\}^{(\gamma+1)/[2(\gamma-1)]}} \qquad (6)$$

For sonic conditions, if γ is assumed to be 1.4 and R is assumed to be 287 J/kg-K, the MFP is equal to 0.04042. It is assumed that the pressure readings from the PDR chamber represent total pressure, and the total temperature is room temperature (293.15 K or 68^0 F). If the cross-sectional area for the throat is 0.1 square inches or $6.45*10^{-5}$ square meters, the mass flow for the PDE is 0.032 kg/sec.

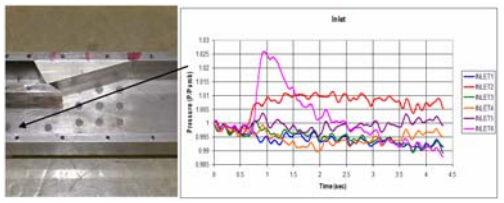

Figure 6: Static steady state inlet readings

In looking at the data for the transducer readings in the inlet, the majority experience a slight drop in pressure ratio, once the ejector is started, to an average value of 0.995. Due to the fact that the inlet is exposed to the ambient air in the room, the ambient pressure is also the stagnation pressure for these transducers. The drop in pressure indicates that some of the total pressure is converted to dynamic pressure. This means that the ejector is entraining air as it was designed to do. Referring again to the compressible isentropic flow equations, a pressure ratio of 0.995 indicates that the flow in the inlet is at Mach 0.085.

To look at the entrainment mass flow, the same equation is applied using the flow properties of the ambient air in the room. The cross-sectional area for the inlet is 7.0 square inches (4.0 inches by 1.75 inches) or 0.00452 square meters. If the air is assumed to have a temperature of 293.15 K (68^0 F) as stated earlier and a ratio of specific heats of 1.4, the mass flow for the inlet is 0.152 kg/sec.

Coming into the mixing interface, the flow from the inlet initially does not vary significantly. The first transducer on the bottom row settles on a pressure ratio of about 0.995, just like the average reading from the inlet transducers. For the row just above that, the first

transducer indicates that the pressure ratio is 0.986 after transient effects have decayed. This indicates that the flow increases velocity at this location. The second and third transducers in both rows show a rise in pressure above ambient conditions. This rise in pressure is a realization of energy being imparted to the secondary flow from the ejector. It is not known exactly how much stagnation pressure is gained by the secondary flow, and this precludes making a prediction in velocity. Kerrebrock [9] made some estimates of how much stagnation pressure is gained in a mixing chamber, but these estimations can only be made far downstream where the flow properties are homogenous throughout the system. Based upon the static pressure plots, it would not be valid to make this assumption at this location. The model further assumes constant cross-sectional area which the presence of the CD nozzle insert invalidates.

The transducers at the top of the mixing interface experience the most radical pressure ratios external to the PDE chamber. As stated earlier, it was not certain that the first transducer on the top row would be blanketed out by the CD nozzle insert, but according to the data gathered here, the data it produces are consistent with the rest of the system. It shows a large pressure ratio drop to a value of approximately 0.87 after the ejector is started. This reading agrees quite well with the fact that it is the transducer location that is closest to the nozzle throat where flow speed is still quite large. As the flow continues down stream, the flow velocity continually reduces, as is verified by the second and third transducer at the top of the mixing interface. Each transducer shows less decay in pressure ratio than the transducer before it, validating the fact that the flow is indeed subsonic as previously thought. If it were supersonic, the flow would undergo a progressive decrease in pressure as it continued to expand to higher Mach numbers.

As for the row of transducers below that, a similar, but less drastic trend is seen. The first transducer sees the greatest drop in pressure with the last transducer seeing the least. Again, this validates that the flow is subsonic.

Unfortunately, due to the presence of a shock wave in the system, as validated by the pressure readings in the upper portion of the mixing interface, it cannot be assumed that the stagnation pressure in the flow path of the primary flow is equivalent to what is in the PDE chamber. Because this is not known, a true assessment of the velocity can not be made as was the case in the lower portion of the mixing interface. Only a prediction of the trend based upon knowledge of compressible flow theory can be made.

Understanding that total pressure would be higher at the top of the mixing interface than below the splitter plate coupled with the transducer readings, it is reasonable to guess that the flow velocity at the aft end of the mixing interface decays from top to bottom. Even though the bottom is the point of lowest velocity, it is assumed that the flow speed is slightly greater than that of the inlet as the primary flow accelerates it across the shear layer. Since pressure readings confirm that the system is subsonic in the mixing interface, a shock system as seen in figure 7 is anticipated. Since the area expansion is great, it is expected for the flow to detach from the walls with a shock induced flow separation. This translates into a much thicker shear layer area than would typically be seen if the flow were fully attached.

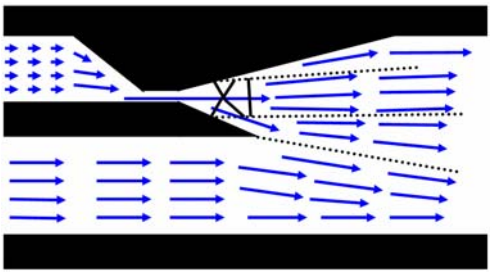

Figure 7: Estimated velocity vector field for static steady state tests

Because accurate information of velocity can not be extracted at the exit plane being examined, thrust augmentation can not be determined by conventional means. However, from the analysis done on the PDE and the inlet, there is an entrained mass flow to primary mass flow ratio, β, of 4.682. If this is value is inserted into the Porter and Squyers [3] method for solving for thrust augmentation (2), it is determined that the steady-state ejector has a thrust augmentation of 1.643.

Mach 0 Low Frequency Run

The low frequency run was set up just like the steady-state run allowing a total post-filtered run time of 4.32 seconds. A simple count of the pulses in the PDE chamber divided by the run time indicates that the frequency is 11.1 Hz. The peak pressure ratio at the crest of each pulse rises to a maximum value of 2.8. This peak pressure in the PDE is almost ½ an atmosphere over the steady-state case. This is due to the fact that the PDE is slightly under-damped as discovered in the steady-state run and because the valve

closing and opening at a much higher frequency does not allow the much slower frequency response of the system time to equalize.

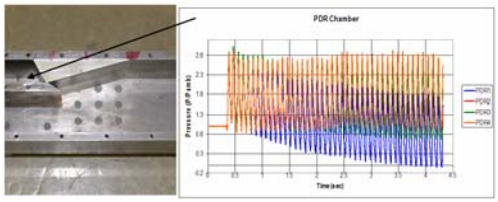

Figure 8: Static low frequency PDE readings

A temperature drift effect is seen in the first pressure transducer position. This is assumed because the effect is severe enough to cause it to output negative values. This validates that this is an instrumentation effect and not an accurate reading. This effect will be discussed in greater detail in the supersonic tests.

Because there is no noticeable time lag in pressure readings from front to back, the assumption that the flow is stagnant in the chamber is still valid. Adding a degree of complexity to the steady-state run, the value of the stagnation pressure at the mixing interface is made less certain by the fact that the total pressure in the PDE fluctuates from ratio values of 0.9 to 2.8. Again from Mattingly [8], due to the very large expansion ratios seen in the CD nozzle, it is valid to assume that the throat is experiencing sonic conditions for the entire cycle.

After removing the drift in the first transducer location, the remaining time averaged pressure ratio is 1.65, much lower than the steady-state case of 2.18.

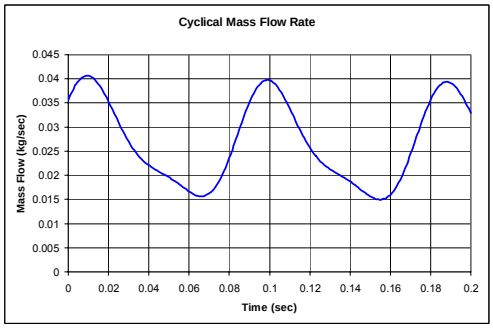

Figure 9: Primary mass flow plot for low frequency static test

Determining a mass flow rate now becomes increasingly complex due to the fact that the pressure changes with respect to time. However, if the same assumptions are made as in the steady-state run with the exception that the total pressure changes with a function of time according to the transducer data, a reasonable value for mass flow can be extracted, again, via the mass flow parameter.

A time-averaged mass flow extracted from the calculated data, taken over 3.32 seconds of steady run time indicates that the PDE is pumping at a rate of 0.024 kg/sec. This is significantly lower than the mass flow calculated for the steady-state ejector as expected since the flow is stopped for a portion of the cycle unlike the steady-state case.

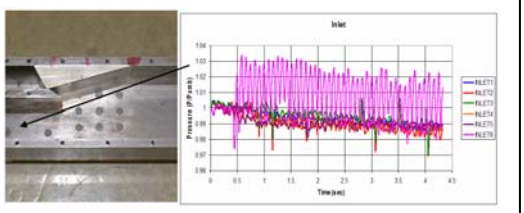

Figure 10: Static low frequency inlet readings

For readings in the inlet, the first five transducers in the inlet as shown in figure 10 all see a drop in pressure ratio to an average value of 0.988 after the motor is activated. Again assuming that the ambient pressure is a good value for total pressure and using isentropic flow properties, it can be determined that the flow in the inlet is traveling at Mach 0.130. This indicates that a pulsed ejector is inducing a greater impact on the secondary flow. This translates to an entrained mass flow of 0.247 kg/s making the same assumptions on the ambient air.

Even though the transducers do respond to the pulses, this response is limited to negligible changes of the same frequency in pressure ratio. This proves that these effects do not propagate upstream, and the unsteady nature on the PDE has no macroscopic effect on the secondary flow path other than inducing greater velocity, and subsequently, greater mass flow.

Information from the data in the lower region of the mixing interface is similar to the data gathered for the steady-state test. The first two transducers see a drop in pressure with the lower transducer agreeing well with the pressures in the inlet. It maintains an average pressure ratio value of 0.988 giving it the same Mach 0.130 flow speed assuming that total pressure is the same as ambient conditions.

Upon inspection of the second and third pressure transducer locations, a similar trend to that of the steady-state run is seen. Again, velocity can not be determined as the actual stagnation information remains undetermined for the same reasons stated earlier.

The pressure information from the upper region of the mixing interface validates the fact that the flow is subsonic entirely aft of the nozzle as before. As the flow moves front to back, the pressure ratios get less dramatic as the flow continues through the growing cross-sectional area.

Looking at the top row, the first transducer experiences a cyclical drop in pressure to values as low as 0.84. The other two transducers, like the first, have a very steady oscillating response to the PDE flow but with much smaller amplitude. The flow in the row below it does show responses to the pulsed jet, but these responses are noisy and less ordered like the rest of the system. This means the effects of the pulsating flow are greatest along the upper surface of the primary flow and dissipate further down the mixing area.

With this information, it is still difficult to predict stagnation pressures in the flow, and, in turn, velocity. From the data available, it can be said that the upper wall of the model experiences the most consistent cyclical change in pressure. Without having an accurate assessment of total pressure, it is not known how this impacts velocity. With the unsteady flow, it is expected to show "jelly rolls" in the flow, greatly expanding the shear layer in the mixing interface, and it is anticipated that the shear layer will grow more in the direction of the secondary flow due to the average pressure ratio difference between the two flows. Similar to the steady state flow, a shock structure forms in the nozzle of the PDE and detaches it from the wall. As the PDE pulses, the shock will fluctuate making the point of separation change as a function of the cycle. This will expand and contract the primary jet between the shear layers as well.

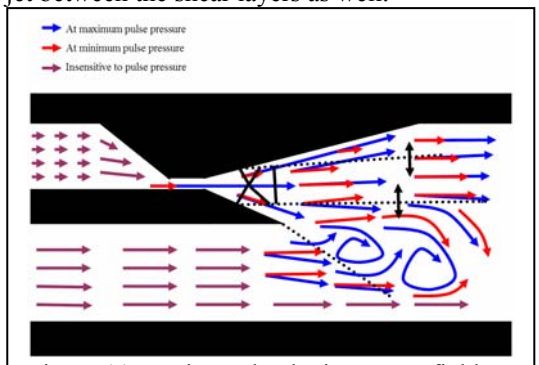

Figure 11: Estimated velocity vector field for static pulsating tests

Again if the entrainment ratio is calculated, it is determined to be 10.29. Using the same method as was used in the steady-state run, a value of 2.00 is predicted for thrust augmentation.

Mach 0 High Frequency Run

For the high frequency run, the driving motor was set to an arbitrarily high frequency and data was sampled. In the PDE chamber, from counting pulses over a given length of time, it is determined that the PDE frequency was 22.9 Hz. Unlike the low frequency data, the pressure ratios in the chamber only climb to values of 2.3 and decay to values of 1.3. The reason that these pulses are less dramatic is due to the limits of the rotary valve and the PDE throat. As the valve rotates at higher speeds, there is less time that the valve is in phase. This indicates that a smaller slug of air is allowed through the valve into the system reducing the maximum pressure. Since the PDE is acting more like a storage tank than a duct due to the small throat area, the pressure capacitance of the chamber is not fully depleted before the next cycle either.

Time averaged data from the transducers that do not show drift indicate that the average pressure ratio is 1.79, slightly higher than the low frequency run, but still much less than the steady-state run.

For the high frequency run, taking advantage of MFP and assuming the sonic condition at the throat, the values oscillated between 0.021 kg/sec and 0.034 kg/sec. The time averaged value for mass flow is 0.027 kg/sec taken over 3.32 seconds of steady run time.

Unfortunately, the pressure readings from the inlet do not agree as well as in the low frequency test. In fact, the first, fourth, and fifth transducer see no net effect before and after the ejector is started. If an average of all transducers is taken, a pressure ratio of 0.995 is seen. This is identical to the steady-state run, indicating that the flow is Mach 0.085 under the standard assumptions. Since that is the case, it yields the same value for entrained mass flow of 0.152 kg/sec.

Coming into the mixing interface, the same trends in the steady-state and low frequency tests are apparent. The first transducer on the bottom row settles on a pressure ratio of about 0.995 and the first transducer on the row above indicates that the pressure ratio is 0.985 at that location.

For the top row, the transducers again see the most ordered response to the flow. The values for the first transducer location are somewhat attenuated due to the lower amplitude in the PDE chamber only reaching pressure ratios of 0.885. The transducers again validate

the fact that the flow is subsonic in the presence of a growing cross-sectional area.

The row below it shows a small pressure drop upon initiation of the PDE. All values seem to decay only slightly to 0.998.

Considering all of the data presented, the high frequency run is more of a hybrid of the steady-state and low frequency runs, containing distinct elements from both. The induced effects on the secondary flow are very close to the steady-state run, but the large velocity gradients along the upper wall of the model are more consistent with the low frequency fluctuations. It is safe to say that if the net effect on the secondary flow of the higher frequency PDEE pulses is roughly equivalent to that of the steady-state ejector, the pulsed jet remains more efficient. This is by virtue of the fact that the primary flow in the pulsed jet has a much smaller average mass flow due to the periodic starting and stopping of the flow.

Using Porter and Squyers [3], the β term is calculated to be 5.63. When applying that to Eq.1.5, a thrust augmentation of 1.72 is calculated.

Supersonic Runs

For the supersonic runs, the data acquisition system was turned on prior to the activation of the motor and the wind tunnel so there would be a portion of data at the beginning of the run that indicates stagnant conditions of the system. The run time of the system was increased to 10.24 seconds to allow plenty of time for the wind tunnel to ramp up to supersonic conditions and capture the entire supersonic portion of the data. Once the data was filtered and manipulated, only 4.5 seconds was extracted for further examination.

Much like the frequency of the control motor, the true Mach condition of the flow can only be backed out from the wind tunnel data after the run. If the velocity in the plenum chamber is assumed to be slow enough to represent stagnation conditions, the pressure ratio (p/p_t) in the test section is approximately 0.090. Isentropic flow properties reveal that the actual speed of the tunnel in the test section is Mach 2.23.

The pressure transducers in the PDE chamber showed similar results to the data from the low frequency runs as expected. Once again, counting the pulses over time indicates that the run operated at a 13.6 Hz rate. Mass flow is calculated in the same manner as was done in the Mach 0 tests, and a total primary mass flow of 0.024 kg/sec was obtained.

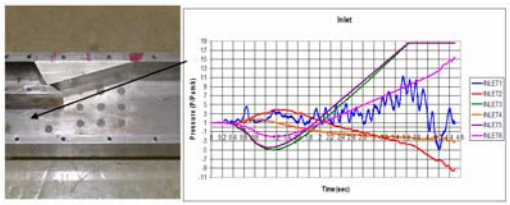

Figure 12: Supersonic low frequency inlet readings

In the inlet, the data becomes increasingly difficult to interpret. Three of the transducers (third, fifth, and sixth) upon initiation of the wind tunnel drop in pressure and then rise to some saturated value where they stay for the remainder of the run. The data is clearly erroneous, but there has been no reasonable explanation for this behavior. The fact that they endure no fluctuation as they saturate indicates the possibility of transducer failure. Careful documentation during the test, as will be seen later indicates that the problem is unique to the transducer and re-appears in the mixing interface information as well. The first transducer experiences some excitation, but the reason for this may be similar to the third transducer in the inlet in which the supersonic flow vibrated it loose inside its pressure tap.

The remaining two transducers are the only ones from which meaningful data can be extracted. Both show a steady rise upon the acceleration of the wind tunnel, but then show an almost linear decay until the wind tunnel deceleration in the test. This linear decay, even though different for the two transducers, is the most well behaved example of transducer drift seen. It becomes obvious when considering the flow properties of the wind tunnel. Isentropic flow properties state that the wind tunnel experiences a temperature ratio (T/T_t) of 0.508 for the associated pressure drop. Temperature readings in the plenum chamber indicate that the flow is at 67^0 F or 19.4^0 C (292.6 K), indicating that the flow in the test section is at -192.1^0 F or -124.5^0 C (148.6 K) which is well below the specification ratings for these transducers. Essentially the transducers are being super-cooled as a result and the pressure readings reflect that dipping into negative pressure ratios. The transducers have a temperature sensitivity of $0.36\%/^0$ C. Given the entire range of the temperature drop, this equates to a 51.84% degradation in signal from the transducer.

An approximation of the effect can be made by looking at the properties of the transducers. The total range of the transducers is ±249.85 psig

or a total of 499.70 psig. If that is the case, a 51.84% reduction in signal would attenuate that to a total range of 259. 04 psig. The attenuated signal must be expanded from the absolute lowest reading, although physically impossible, across the entire original range in the following manner.

$$p_{actual} = \frac{(p_{reading} - p_{\min})}{w_{trans}\Delta T} - \frac{R_{total}}{2} \tag{7}$$

For a total pressure range of 499.7 psig, a minimum pressure reading of -249.85 psig, and the given sensitivity, the following transducer map can be constructed correlating pressure readings and temperature effects.

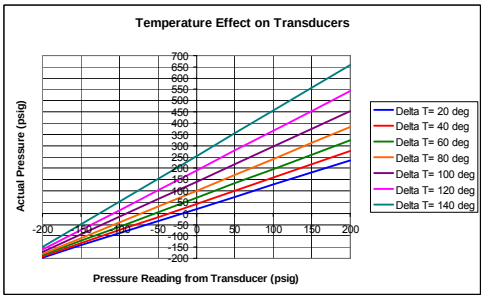

Figure 13: Temperature effects on pressure transducers

The important thing to note is there are no major departures from this near-linear decay during the steady-state run time of the tunnel. That indicates that the flow is traveling though the inlet at a constant supersonic rate with no propagations up or down stream.

If in fact the inlet is experiencing the same Mach number as the wind tunnel, a calculation of mass flow can be done using the MFP. Bear in mind that the total pressure and total temperature are no longer ambient conditions, but the conditions inside the plenum chamber. With that indicated, the mass flow for the inlet is 4.36 kg/sec.

The same behavior is also seen in the transducers in the lower region of the mixing interface. A small pressure rise at the beginning of the test occurs followed by a steady decay. In addition to the fact that the data agrees well with the useable data in the inlet, the second row of transducers shows more of a decay in pressure readings than the first. This might indicate that on average, the flow at this location is colder, and that an isentropic expansion is bending the secondary flow into the primary flow. This explanation also agrees with [Kerrebrock [9]] in which the total pressure ratios ($p_{t/secondary}$/ $p_{t/primary}$) is approximately 8.

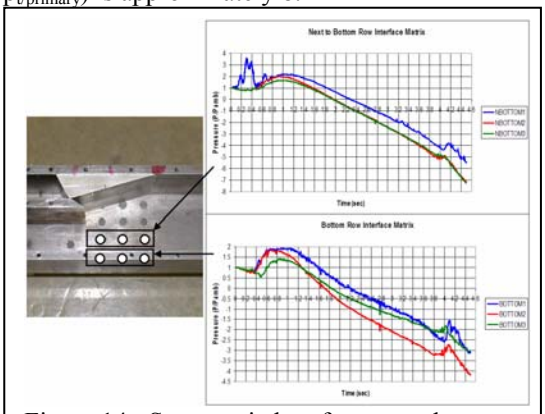

Figure 14: Supersonic low frequency bottom mixing interface readings

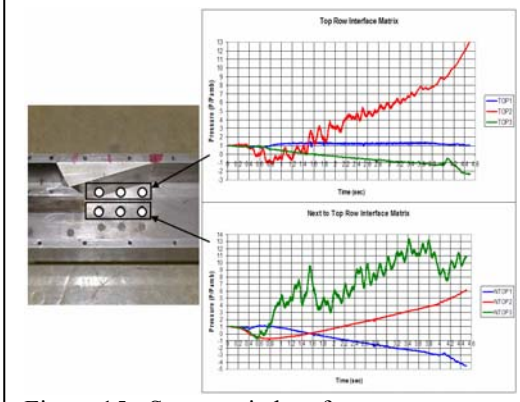

Figure 15: Supersonic low frequency top mixing interface readings

In the upper region of the wind tunnel the same transducers that increased to saturation limits in the inlet cause the same problems here. The first transducer in the top row is the only location outside the PDE that indicates the presence of a pulsed flow. It further does not drift, indicating that the flow in this region is entirely from the primary flow. The remaining two transducers see a minimal transducer drift indicating that the two flows are mixing at these locations.

Upon inspection of the high frequency run at supersonic conditions, there was virtually no change in the data. This is due to the fact that the difference in mass flow from the primary to the secondary is so high that the effects of the PDE are diminished greatly. With that in mind, it is anticipated that the secondary flow actually expands in a near-isentropic nature into the primary flow. The expansion fan is reflected off the lower surface of the model to turn the flow back into the axial direction. Because of transducer drift and a lack of total pressure

information, it is hard to determine the magnitude and impact of this expansion on the system. It is also anticipated that this expansion/shock structure extends far past the last column of transducers.

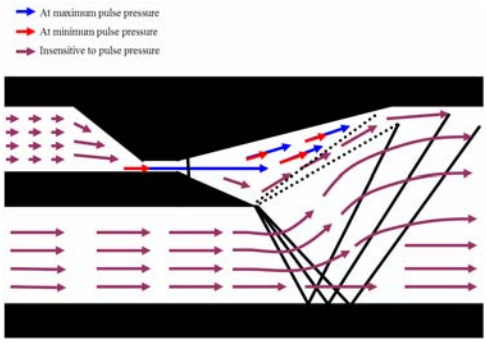

Figure 1: Estimated velocity vector field for supersonic tests

Unfortunately, due to the fact that the flow is moving relative to the inlet, it can not be assumed that the air flowing through it is entrained mass. Further, this negates the ability to use the Porter and Squyers [3] method for determining thrust augmentation.

CONCLUSIONS AND RECOMMENDATIONS

Table 1: Results from experimental runs

Run	Freq.	Primary Mass Flow	Secondary Mach	Secondary mass flow	β	Φ
	Hz	kg/sec	NA	kg/sec	NA	NA
Mach 0 Steady-state	0.0	0.032	0.085	0.152	4.68	1.64
Mach 0 Low Freq.	11.1	0.024	0.130	0.247	10.29	2.00
Mach 0 High Freq.	22.9	0.027	0.085	0.152	5.63	1.72
Supersonic Low Freq.	13.6	0.024	2.23	4.36	Unkwn	Unkwn
Supersonic High Freq.	28.6	0.027	2.23	4.36	Unkwn	Unkwn

All Mach 0 tests indicate that unsteady ejector performance is better than steady performance as was expected [Paxson and Wilson [4]]. Quantifiable results for thrust augmentation were obtained via the Porter and Squyers [3] method, but proved to be slightly too optimistic to be trusted. A more accurate prediction of thrust augmentation could not be used due to the lack of knowledge of total pressure in the mixing interface, but it was determined that the secondary flow is relatively insensitive to the primary flow fluctuations, and higher frequency ejector rates drive the system to results closer to steady-state.

As for supersonic test results, there was little to no effect on the secondary flow from the primary flow due to the large mass flow ratio between the secondary flow and the primary flow. It is anticipated that this will be one of the limiting factors on what speed mode 1 of the propulsion concept [Munipalli et al. [1]] will be able to attain as the primary flow will be fixed as the secondary flow will be able to change drastically.

Despite the issues with inaccurate mass flows, this set of runs gives a picture as to what an actual detonating ejector will produce during some benign part of the cycle such as the purge air fill. The system can also be viewed in reverse, and provide insight into what a detonation flow would do in a slow subsonic condition. If the secondary flow was the primary and vice versa, this sort of trend is expected as a high-pressure detonation expands into a slow-moving flow. The major difference would be the lack of temperature effects since that phenomenon would be associated with a very hot gas.

It is also important to note that, the inlet did truly experience supersonic flow throughout its length with no perturbations propagating upstream.

After an uncertainty analysis, it was determined that all mass flows are accurate to within 0.1 kg/sec on the secondary flow and 0.01 for the primary flow.

REFERENCES

[1] Munipalli, R., Shankar, V., Wilson, D.R., Kim, H.Y., Lu, F., Hagseth, P.E., "A Pulsed Detonation Based Multimode Engine Concept," AIAA 2001-1786, 2001.

[2] Bussing, T. and Pappas, G., "Pulse Detonation Engine Theory and Concepts," *Developments in High-Speed-Vehicle Propulsion Systems*, edited by Murthy, S. and Curran, E., Vol. 165, Progress in Astronautics and Aeronautics, AIAA, Reston, VA, 1997.

[3] Porter, J.L., and Squyers, R.A., "A Summary/Overview of Ejector Augmentor Theory and Performance," ATC Report No. R-91100/ 9CR-47A, Vought Corporation Advanced Technology Center, Dallas, TX, 1979.

[4] Paxson, D.E. and Wilson, J., "Unsteady Ejector Performance: An Experimental Investigation using a Pulsejet Driver," AIAA 2002-3915, 2002.

[5] Heiser, W.H., and Pratt, D.T., "Hypersonic Airbreathing Propulsion," AIAA Educational Series, 1994.

[6] Matsumoto, J., "Design and Testing of a Subscale Supersonic Aeropropulsion Wind Tunnel," Master of Science in Aerospace Engineering Thesis, University of Texas at Arlington, Arlington, TX, 2000.

[7] Meyers, J.M., "Performance Enhancements on a Pulsed Detonation Rocket,"

Master of Science in Aerospace Engineering Thesis, University of Texas at Arlington, Arlington, TX, 2002.

[8] Mattingly, J.D., "Elements of Gas Turbine Propulsion," 2nd Ed., McGraw-Hill, Inc., 1996.

[9] Kerrebrock, J.L., "Aircraft Engines and Gas Turbines," 2nd Ed., The MIT Press, 1992.

[10] Holman, J.P., "Experimental Methods for Engineers," 6th Ed., McGraw-Hill, Inc., 1994.